Original Article

Prevention and Mitigation of Debris Flow Hazards by Using Steel Open-Type Sabo Dams

Joji SHIMA[1], Hiroshi MORIYAMA[2], Hiroshi KOKURYO[2], Nobutaka ISHIKAWA[2] and Takahisa MIZUYAMA[3]

[1] Sabo & Landslide Technical Center (4-8-21 Kudan-Minami, Chiyoda-ku, Tokyo 102-0074, Jaapan)
[2] Research Association for Steel Sabo Structures (2-7-4 Hirakawa-cho, Chiyoda-ku, Tokyo, 102-0093, Japan)
E-mail: cgishikawa@m4.dion.ne.jp
[3] National Graduate Institute for Policy Studies (7-22-1 Roppongi, Minato-ku, Tokyo, 106-8677, Japan)

This paper presents the findings of an investigation on the prevention and mitigation of debris flow hazards by using steel open-type dams. First, the actual cases of trapping hazardous debris flow by steel open-type dams were surveyed. Through a field survey of actual cases, we classified them into four distinct scenarios based on the trapping type of debris flow: Scenario A (wooden debris + rocks + sediment), Scenario B (wooden debris + sediment), Scenario C (rocks + sediment) and Scenario D (wooden debris only). Second, recent trapping cases on protection and mitigation by various steel open dams were introduced. Third, trapping scenarios A, B, C and D were confirmed by performing physical model tests. Finally, a safety check of a steel open dam against a large rock was verified by two impact analyses, the finite element method (FEM) impact analysis using ANSYS Autodyn software, and the three dimensional (3-D) impact frame analysis.

Key words: steel open dam, debris flow hazards, trapping scenario, model test, impact analysis

1. INTRODUCTION

Recently, abnormal weather has given rise to debris flow hazards in mountainous areas in Japan. Since 1980, many steel open-type Sabo dams (hereafter, "steel open dams") have been constructed as defensive measures against debris flow hazards [*Steel Sabo Structure Committee*, 2009; *Kasai et al*., 2006; *Ono et al*., 2004]. A steel open dam is composed of steel pipe components, which usually allow water, soil and small pieces of gravel to flow downstream through gaps in the steel structure. However, it functions to block rocks and wooden debris during debris flow. In Japan, the design guidelines for dams were revised [*National Institute for Land and Infrastructure Management*, 2007] such that a steel open dam should be basically constructed in the debris flow section as a countermeasure against debris flow and wooden debris.

This paper presents an investigation into the prevention and mitigation of debris flow hazards by using steel open dams. First, we surveyed actual cases of the trapping of hazardous debris flow by steel open dams. Through our field survey [*Moriyama et al*., 2008; 2010; 2011; 2013; 2014; *Yoshida et al*., 2011; 2012; *Ohsumi et al*., 2012], we classified the trapping cases into four distinct scenarios (**Fig. 1**). The relationship of rock diameter and gap ratio was examined in scenarios A and C. Second, recent trapping cases on protection and mitigation by various steel open dams were introduced. Third, these scenarios were confirmed by conducting physical model tests. Finally, a FEM impact analysis using ANSYS Autodyn and a 3-D impact frame analysis were performed to check the safety of a steel open dam against a large rock.

2. TRAPPING SCENARIOS

Thirty-nine trapping cases of through steel open dams, since 1992, were investigated. From this field survey, we classified these trapping cases into four scenarios based on the trapping type of debris flow, as shown in **Fig. 1**.

2.1 Relationship between trapped number and scenario

Twenty traps were categorized as Scenario A, which equates to 51% of the total traps. This proved to be the most effective trapping scenario of the

(a) Scenario A
(wooden debris +rocks +sediment)

(b) Scenario B
(wooden debris +sediment)

(c) Scenario C
(rocks +sediment)

(d) Scenario D
(wooden debris only)

Fig. 1 Trapping scenarios

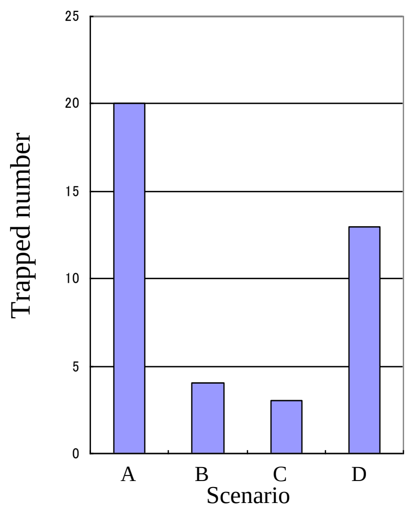

Fig. 2 Trapped number - Scenario relation

four, as shown in **Fig. 2**.

Four traps were categorized as Scenario B, which equates to 10% of the total traps. A number of recent cases in Mt. Aso, Kumamoto Prefecture, Izu-Oshima Island and the Hachiman-tani River, Yamaguchi Prefecture fall into this scenario. These cases will be discussed in more detail later.

The number of Scenario C cases was limited to three (8%), as this represents a rare case in which rocks and sediment are trapped without wooden debris. On the contrary, 13 cases were categorized as Scenario D, which is relatively common, representing 31% of the total cases. Since Scenarios A, B and D have all trapped wooden debris, it can be confirmed that a steel open dam has the structural characteristics required to trap debris flow,

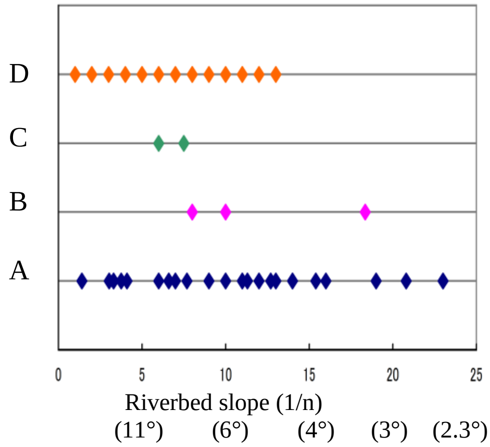

Fig. 3 Scenario - riverbed slope relation

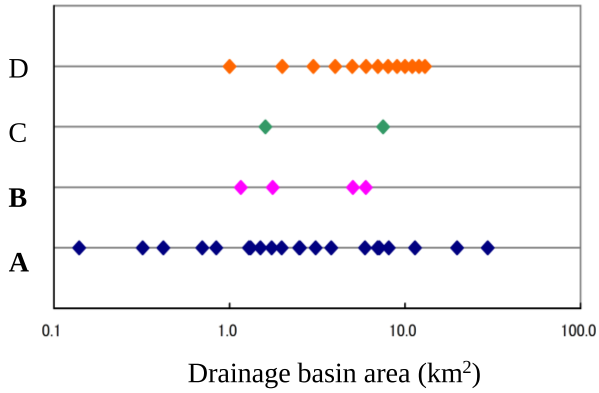

Fig. 4 Scenario- drainage basin area relation

including wooden debris, caused by the opening of a spillway.

2.2 Relationship between trapping scenario and riverbed slope

The relationship between the trapping scenario and the riverbed slope was plotted as shown in **Fig. 3**. The most flexible and effective trapping scenario was Scenario A, which was spread across a riverbed slope range of 1/24 - 1/2 (2.4 - 29°). The next most effective trapping scenario was Scenario D covering a slope range of 1/10 - 1/2 (6 - 29°). Scenario C was limited to a slope range of 1/7 -1/6 (8 - 10°), while Scenario B covered a slope range of 1/18 - 1/8 (3 - 7°).

2.3 Relationship between trapping scenario and drainage basin area

The relationship between the trapping scenarios and the area of the drainage basin is shown in **Fig. 4**. It was found that Scenario A was spread over an area of 0.2–80 km^2, while Scenario B and Scenario C were limited to areas of 1.0–10 km^2, which occurred in the narrow basin area of elevation less than about 500 m.

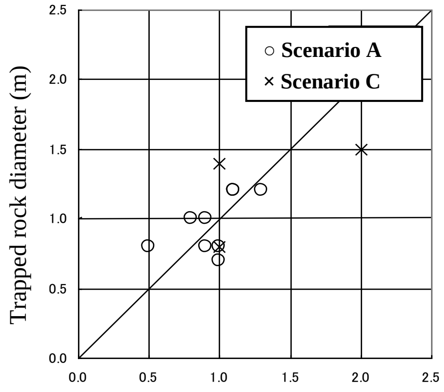

Fig. 5 Predicted - trapped rock diameters relation

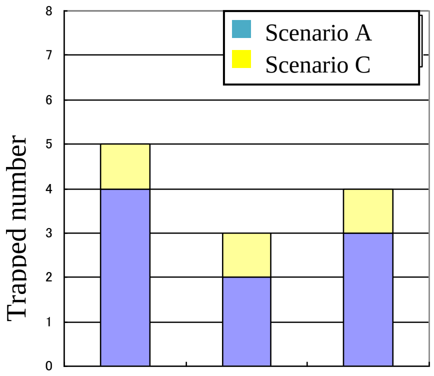

Fig. 6 Trapped number - gap ratio relation

(a)Trapped wooden debris, rocks and sediment

(b) Protection of houses in down stream

Fig. 7 Scenario A in Kumamoto

2.4 Relationship between predicted and trapped rock diameters

Figure 5 shows the relationship between predicted and trapped rock diameters in Scenarios A and C. The predicted and trapped rock diameters mean the maximum diameter (D_{95}) before the construction and after the event of debris flow, respectively. The D_{95} is found to be the rock diameter corresponding to 95% of the cumulative curve of rock size distribution in which more than 200 rocks were measured on-the-spot. It can be seen that the trapped rock diameter closely coincides with the predicted rock diameter, with the exception of one case in Scenario C in which the predicted rock did not appear in the actual case.

2.5 Relationship between trapped number and gap ratio of steel open dam

Figure 6 represents the relationship between trapped number and the gap ratio (W/D_{95}, W: gap width, D_{95}: maximum rock diameter). It was found that the gap ratio of eight trapping cases was less than or equal to 1.5 in Scenarios A and C, while the gap ratio of the four remaining cases was 2.0. This data indicates that it is possible to trap large rocks in the debris flow, even if the gap ratio is 2.0.

3. PROTECTION AND MITIGATION OF ACTUAL CASES

3.1 Scenario A (wooden debris + rocks + sediment)

Figure 7 (a) shows a typical trapping case of a steel open dam which trapped wooden debris, rocks and sediment in the Kitasato river, Kumamoto in July 2005 [*Moriyama et al*., 2008]. This debris flow occurred due to the collapse of the slope on one side of the dam caused by downpour as a result of a typhoon.

Although a number of the rocks were stopped by the concrete dams upstream of this dam, most of wooden debris, rocks and sediment overflowed these dams and were trapped by the steel open dam. Therefore, most of the houses downstream were protected against debris flow including wooden debris, as shown in **Fig. 7 (b)**.

Figure 8 (a) shows a further Scenario A case of a steel open dam with steel cell dams in the Funaishi river, Kagoshima Prefecture, in August

(a)Trapped rocks, wooden debris and sediment by steel open dam

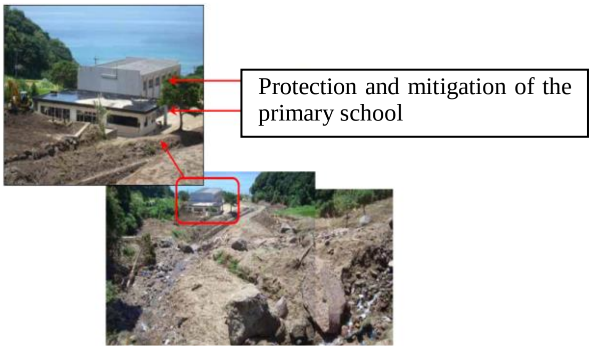

(b) Downstream in the Funaishi river

Fig. 8 Scenario A in Kagoshima,2007

(a) before debris flow

(b) after debris flow

Fig. 9 Scenario B in Izu-Oshima island,2013

2007. The primary school downstream was protected, as shown in **Fig. 8 (b)**. Although the steel cell dams were damaged and deformed by the debris flow, the steel open dam itself was not damaged.

3.2 Scenario B (wooden debris + sediment)

Figure 9 (a) and **(b)** show the pictures taken before and after the debris flow caused by Typhoon No. 26 in Izu-Oshima Island, 2013.

The debris flow was considered to be a mudflow of volcanic debris, including wooden debris, likely caused by the surface failure of the slope. Debris excavation work determined that there were no rocks in the debris flow and, as such, this trapping case was classified as Scenario B.

Figure 10 (a) shows a further Scenario B trapping case in the Hachimantani river, Yamaguchi Prefecture, in July 2009 [*Yamaguchi et al*., 2011]. Eight months later, during excavation work, a large amount of wooden debris was accumulated, as

(a) Trapped wooden debris

(b) Excavated wooden debris

Fig. 10 Scenario B in Yamaguchi,2009

(a) Down stream of dam

(b) Upper stream of dam

Fig. 11 Scenario C in Rishiri island,2006
(gap width =1.4 m)

shown in **Fig. 10 (b)** [*Yoshida et al*., 2011]. Therefore, these steel open dams were considered to be highly effective for the prevention and mitigation of the damage caused by the wooden debris downstream.

3.3 Scenario C (rocks +sediment)

Figure 1 (c) illustrates a typical case of Scenario C in Rishiri-island, Hokkaido in October 2006 [*Tsutsui et al*., 2009]. The drainage basin area and riverbed slope of this steel open dam were 4.5 km^2

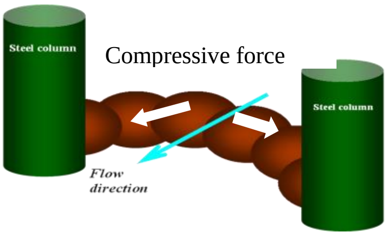

Fig. 12 Arch action

Fig. 13 Scenario C
(gap width = 2.4 m)

Fig. 14 Scenario D (wooden debris only)

(a) Volume 10% of wooden debris

(b) Volume 20% of wooden debris

Fig. 15 Scenario A model test

and 1/7.5 (7.6°), respectively.

Figure 11 (a) and **(b)** indicate the appearance of the downstream and upstream areas of the dam, respectively. It was found that there were no outflow rocks downstream, and that the soil sediment was accumulated upstream of the dam.

Although the gap width of the dam was 1.4 m, it trapped rocks with diameters of 0.5-1.0 m, as well as soil sediment. This trapping mechanism may be due to an arch action in which compressive forces arise as a result of rocks pushing against each other, as shown in **Fig. 12**.

Figure 13 shows a further example of trapped rocks and sediment (Scenario C). Although the gap width of this dam was 2.4 m, rocks with diameters of 0.85-2.0 m were trapped due to arch action.

3.4 Scenario D (wooden debris only)

Figure 1 (d) and **Fig. 14** illustrate Scenario D in which a steel open dam trapped wooden debris only. This is useful for protection and mitigation against wooden debris hazards.

4. MODEL TEST

4.1 Scenario A model test

Scenario A model tests were conducted with wooden debris volume percentages of 10% and 20% at a gap ratio of 1.0, as shown in **Fig. 15** [*Katsuki et al.*, 2013]. In this model test, the scaling factor was 1/50 and the specific gravities of wooden stick (diameter = 6 mm, length = 120 mm) and balls (rock model diameters of 5,10,15,30 mm) were 0.95 and 1.9, respectively. For the 10% case, the open area was blocked by wooden debris and accumulating successive rocks, as shown in **Fig. 15 (a)**. For the 20% case, all wooden debris was trapped in front of the steel open dam and, therefore, the rocks were accumulated backwards, as shown in **Fig. 15 (b)**.

4.2 Scenario B model test

In order to investigate Scenario B, the model test was performed by using a wooden debris model with steel wool, as shown in **Fig. 16** [*Tateishi et al.*, 2015]. The reason why the steel wool was used is to express the flexible root, as it was seen by trapping wooden debris in Izu-Oshima island in **Fig. 9**. In this case, approximately 80% of the sand (sediment) was trapped due to the effect of the flexible root (steel wool).

4.3 Scenario C model test

In order to examine Scenario C, the model test was conducted with the debris flow model consisted of 7760 pieces of gravel which had been screened through a 1-cm sieve, as shown in **Fig. 17** [*Ishikawa et al.*, 2014b].

(a) Trapped wooden debris model and sand

(b) Wooden debris model with steel wool

Fig. 16 Scenario B model test

Fig. 17 Scenario **C** model test

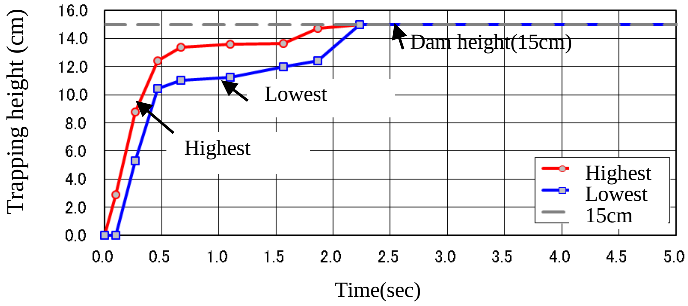

Fig. 18 Trapping height- time relation

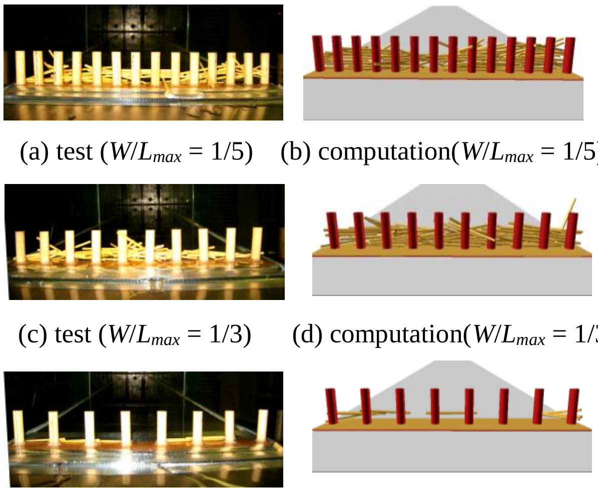

(a) test (W/L_{max} = 1/5) (b) computation(W/L_{max} = 1/5)

(c) test (W/L_{max} = 1/3) (d) computation(W/L_{max} = 1/3)

(e) test (W/L_{max} = 1/2) (f) computation(W/L_{max} = 1/2)

Fig. 19 Scenario D : model test and computation

Figure 18 illustrates the trapping (riverbed) height–time relationship of the debris flow model for a gap of 1.5 cm. The lowest and highest heights of entrapped gravels at the width direction were measured by the video of upstream side from the diagonal direction. These curves express the whole trapping mechanism of gravels. It was discovered that the trapping height was 10 cm to 12 cm at a time of 0.5 s. In this case, the sedimentation occurred rapidly. Therefore, once the first mound of gravel had been trapped by the steel open dam, the remaining gravel quickly accumulated behind it.

4.4 Scenario D model test

In order to examine the effect of opening ratio (W/L_{max}, W: gap width, L_{max}: maximum length of wooden debris) on trap efficiency of Scenario D, model tests were conducted using a wooden debris model (L_{max} = 6 cm and diameter d = 3 mm) as shown in **Fig. 19** [*Shibuya et al.*, 2010]. These model tests were also simulated by developing a distinct element method (DEM) with a new cylindrical stick element to represent wooden debris [*Shibuya et al.*, 2011; *Ishikawa et al.*, 2014a)]. Results clearly show that the trapping efficiency decreases as the opening ratio increases.

5. SAFETY CHECK OF STEEL OPEN DAM

Owing to the torrential rainfall in recent years, it has become necessary to investigate the safety of steel open dams against abnormally large rocks.

Figure 20 (a) illustrates an actual trapping case of a steel open dam against abnormally large rocks (diameters greater than 3 m). **Fig. 20 (b)** shows a further example. Although this dam was able to trap large rocks, the upper part of the dam experienced partial collapse.

Figure 21 shows the largest rock found downstream after debris flow at Nagiso, Nagano Prefecture, in July 2014. This rock had a width of 10 m and length of 3.5 m, and, therefore, an average diameter of 6.7 m.

Therefore, it is necessary to locate abnormally large rocks in the field survey prior to the design process. Following this, it is necessary to develop an impact analysis against these oversized rocks in order to confirm the integrity of the steel open dam.

5.1 FEM impact analysis

A FEM impact analysis was conducted using ANSYS Autodyn software to examine the impact response against a large rock.

Figure 22 shows a steel open dam impacted by a large rock of diameter 3 m with an impact velocity of 8.45 m/s [*Beppu et al.*, 2015]. The computational result shows that the steel open dam was only damaged at the impact point by absorbing the

(a) Trapped large rocks

(b) Trapped large rocks; upper dam collapse.

Fig. 20 Scenario A in Nagano,2014

Fig. 21 Gigantic rock found downstream after debris flow (Weight = about 400ton)

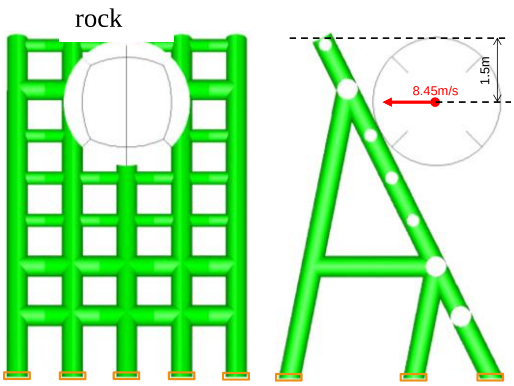

(a) upstream (b)side

Fig. 22 Steel open dam model hit by a rock

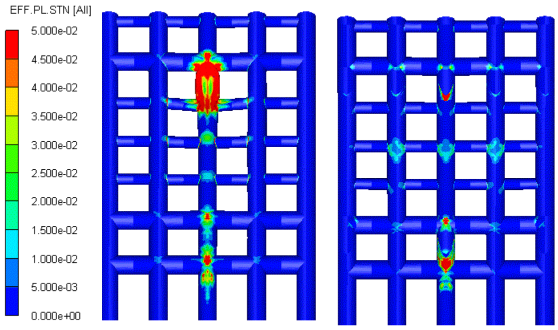

(a) upstream (b)downstream

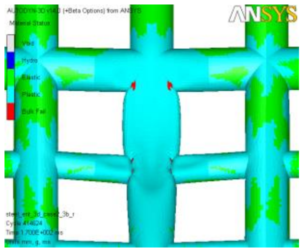

(c) local deformation

Fig. 23 Damage by impact of a rock

kinetic energy of the rock due to local deformation of pipe members, as shown in **Fig. 23**. Therefore, there was no collapse as a whole structure.

5.2 3-D elastic-plastic impact frame analysis

In order to examine the safety of a steel grid type open dam, a 3-D elastic-plastic impact frame analysis was developed [*Ishikawa et al*., 2007].

5.2.1 Ultimate limit state of pipe member

Before performing an impact analysis, the ultimate limit state of a steel open dam was determined by conducting a high speed load test of the pipe member. **Fig. 24** shows the relationship between the dynamic plastic rotation capacity and the diameter-thickness ratio. Herein, the dynamic rotation capacity refers to the occurrence of local buckling of a pipe member.

The high speed load test indicates that a thinner

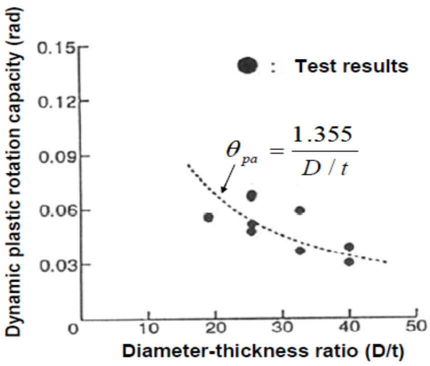

Fig. 24 Relationship between dynamic plastic rotation capacity and diameter-thickness ratio

pipe (large *D/t*) fails more easily by local buckling compared to a thick pipe (small *D/t*) of the same diameter as shown in **Fig. 24**.

5.2.2 Impact analysis of a steel open dam

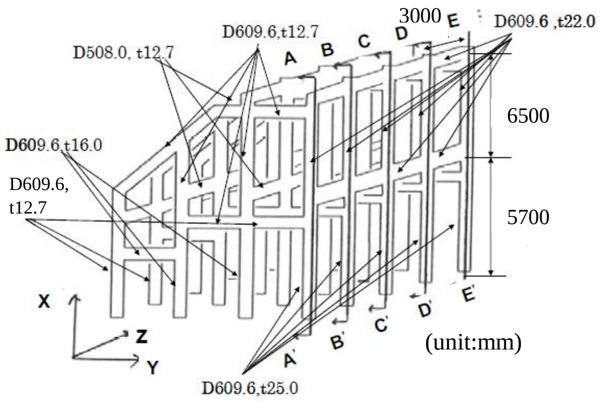

Fig. 25 Steel open grid type dam model

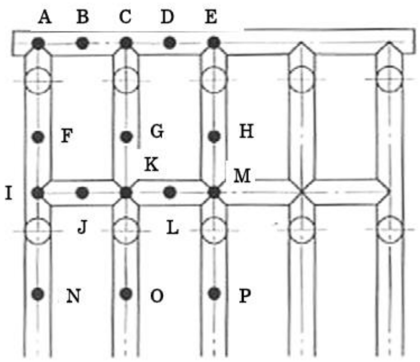

Fig. 26 Different impact points

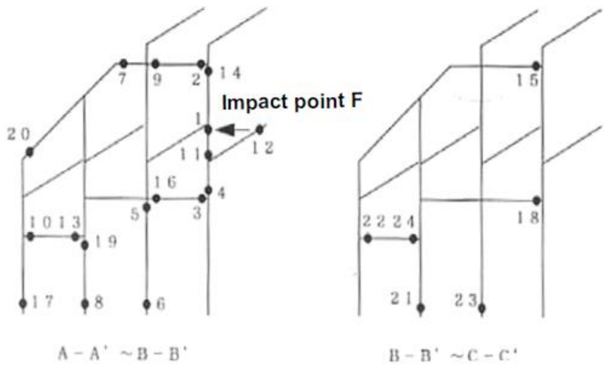

Fig. 27 Plastic hinges at impact point F
(W = 10t, V = 20 m/s)

An impact response analysis was performed for a steel open grid type dam, as shown in **Fig. 25**. The numerical analysis conditions featured a rock with a mass of 10 ton and a velocity of 20 m/s impacting the 16 impact points in front of the dam, as shown in **Fig. 26**.

Plastic hinges formed at impact point F, as shown in **Fig. 27**. Herein, the number in the figure shows the sequence of occurrence of plastic hinges. A plastic hinge is defined as the point where yield stress is reached, and the onset of plastic rotation

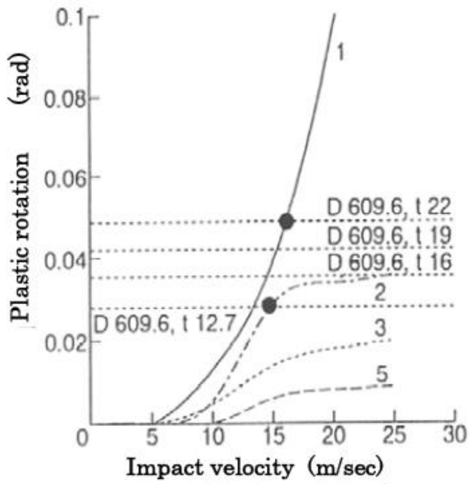

Fig. 28 Plastic rotation – impact velocity relation at impact point F

Table 1 Minimum impact velocity and failure point

Impact point	Min. velocity(m/s)	Failure point
A	18.3	①
B	16.3	③
C	20.0	⑦
D	22.6	⑧
E	21.6	⑬
F	14.6	②
G	15.7	⑨
H	15.6	⑭
I	19.8	④
J	21.3	⑤
K	22.5	⑪
L	21.5	⑩
M	22.5	⑮
N	19.7	⑥
O	19.5	⑫
P	19.6	⑯

has occurred, but has not yet reached capacity which defines the failure criterion.

Figure 28 illustrates the relationship between plastic rotation and impact velocity at impact point F by increasing the impact velocity under a constant rock mass of W = 10 ton. It was found that the plastic rotation of the first plastic hinge (the impact point) was the largest of the plastic hinge rotations. However, the impacted point did not fail, because failure is dependent on the diameter-thickness ratio, as shown in **Fig. 24**. This implies that the failure of a pipe member occurs when the response plastic rotation reaches the plastic rotation capacity.

Therefore, it is of interest that the first failure hinge occurs in the second plastic hinge at an impact velocity of V = 14.6 m/s. This may be the reason why the diameter-thickness ratio (D/t = 48) of the second plastic hinge member may be greater than that of the first (D/t = 28), as shown in **Fig. 24**. That is, the plastic rotation capacity (θ_{pc} = 0.028) of the second plastic hinge member is smaller than that of the first (θ_{pc} = 0.049).

Table 1 shows the minimum impact velocities at the failure points when a rock hit the 16 impact points (A$\rightarrow$P). As a whole structure, the minimum velocity was 14.6 m/s at impact point F, and therefore, the ultimate limit energy E_L is expressed as follows:

$$E_L = \frac{1}{2} mV^2 = 1065\,kJ \tag{1}$$

However, this value is considered to be conservative, because local buckling only occurred at point ② on rock impact with the point F, while no collapse occurred as the whole structure.

6. CONCLUSIONS

The following conclusions are drawn from this study.

(1) From the field survey, the trapping cases of debris flow by steel open dams were classified as four scenarios: Scenario A (wooden debris + rocks + sediment), Scenario B (wooden debris + sediment), Scenario C (rocks + sediment) and Scenario D (wooden debris only).

(2) The most flexible and effective trapping scenario was Scenario A (51% of the traps investigated), which was spread across a riverbed slope range of 1/30 - 1/2 (2 - 29°), and spread over a drainage basin area of 0.2-80 km^2.

(3) Scenario B and Scenario C were limited to areas of 1.0-10 km^2, which occurred in the narrow basin area in the elevation less than 500 m.

(4) Trapped rock diameters closely coincide with the predicted rock diameter.

(5) While the gap ratio of the majority of the trapped rocks was less than or equal to 1.5, rocks with a gap ratio of 2.0 were also trapped.

(6) In the actual Scenario A cases investigated, most of the houses downstream were protected against debris flow including wooden debris.

(7) The actual Scenario B cases investigated show that steel open dams are highly effective for the protection of houses downstream against wooden debris hazards.

(8) An actual Scenario C case showed that a steel open dam trapped rocks with small diameters of 0.5-1.0 m, although the gap width of the dam was set as 1.4 m. This trap mechanism may be due to arch action.

(9) An actual Scenario D case showed that the trapping of wooden debris was useful for the protection of human lives downstream.

(10) Scenarios A, B, C and D were confirmed by conducting model tests (scale factor = 1/50).

(11) The safety of steel open dams was checked by conducting a FEM impact analysis and 3-D frame impact analysis against an abnormally large rock.

It will be necessary for future work to examine the impact strength or absorbing energy of joints or connections between the pipe members of a steel open dam by performing an impact test or high-speed load test.

ACKNOWLEDGEMENT

The authors are very grateful to Professors S. Katsuki and M. Beppu of National Defense Academy and the members of Research Association for Steel Sabo Structures, Japan for their support and cooperation.

REFERENCES

Beppu, M., Matsuzawa, R., Shima, J., Ishikawa, N. and Mizuyama, T. (2015): Computational approach on impact behavior of steel open dam under huge debris flow, Proceedings of Research Meeting of Japan Society of Erosion Control Engineering, No. R6-02, pp. A-82-83 (in Japanese, the title is tentatively translated by the authors).

Ishikawa, N., Hoshikawa, T., Beppu, M. and Mizuyama, T. (2007): Impact response and safety check of steel pipe check dam, Proc. of the 7th International Conference on Shock and Impact Loads on Structures, Beijing, China, pp. 71-81.

Ishikawa, N., Shibuya, H., Katsuki, S. and Mizuyama, T. (2014a): Protective steel structures against wooden debris hazards, Proc. of the 6th International Conference on Protection of Structures against Hazards, 16-17 October 2014, Tianjin, China.

Ishikawa, N., Shima, J., Matsubara, T., Tatesawa, H., Horiguchi, T. and Mizuyama, T. (2014b): Trapping mechanism of debris flow by steel open dams, INTERPRAEVENT 2014 in the Pacific Rim, O-23, 1-6, Nov. 25-28, 2014, Nara, Japan.

Kasai, S., Mizuyama, T. and Inagaki, S.(2006): Debris flow control with steel open-type sabo dams constructed at base point, Journal of Japan Society of Erosion Control Engineering, Technical Note, Vol. 59, No. 4, pp. 48-53 (in Japanese with English abstract).

Katsuki, S., Shibuya, H., Ohsumi, H., Kokuryo, H. and Ishikawa, N. (2013): Trap performance analysis of steel check dam subjected to woody debris by using 3-D DEM, Division A2 (Applied Mechanics), Japan Society of Civil Engineers, Vol. 69, No. 1, pp. 16-29 (in Japanese with English abstract).

Moriyama, H., Ishikawa, N. and Yoshikawa, T. (2008): Excavation of steel open type sabo dam, Proceedings of Research Meeting of Japan Society of Erosion Control Engineering, No. 63, pp. 292-293 (in Japanese the title is tentatively translated by the authors).

Moriyama, H., Ishikawa, N. and Hoshino, K. (2010): A study on the maintenance of steel open type sabo dam, Proceedings of Research Meeting of Japan Society of Erosion Control Engineering, No. 65, pp. 116-117 (in Japanese, the title is tentatively translated by the authors).

Moriyama, H., Ishiakwa, N., Shima, J. and Iizuka, K. (2011): Field survey on steel open type sabo dam at base point, Proceedings of Research Meeting of Japan Society of Erosion Control Engineering, No. 66, pp. 200-201 (in Japanese, the title is tentatively translated by the authors).

Moriyam, H., Kokuryo, H., Yamaguchi, M., Inoue, R. and Shima, J. (2013): Field survey of debris flow trapped by steel open type sabo dam in Mt. Aso, Proceedings of Research Meeting of Japan Society of Erosion Control Engineering (B), No. 68, pp. 168-169 (in Japanese the title is tentatively translated by the authors).

Moriyama, H., Kokuryo, H., Yamaguchi, M., Inoue, R., Ishikawa, N. and Shima, J. (2014): INTERPRAEVENT 2014 in the Pacific Rim, P-33, 1-6, Nara, Japan.

National Institute for Land and Infrastructure Management, Erosion and Sediment Control Division, (2007): Manual of technical standards for designing sabo facilities against debris flow and driftwood, No.365, ISSN. 1346-7328, Research Center for Disaster Risk Management, Ministry of Land, Infrastructure and Transport, Japan (in Japanese).

Ohsumi, H., Kokuryo, H., Shibuya, H., Katsuki, S. and Mizuyama, T. (2012): A study on the field survey of wooden debris and standing trees in Shobara, Hiroshima, Proceedings of Research Meeting of Japan Society of Erosion Control Engineering, No. 6, pp. 706-707 (in Japanese, the title is tentatively translated by the authors).

Ono, G., Mizuyama, T. and Mastumura, M. (2004): Current practices in the design and evaluation of steel sabo facilities in Japan, Proc. of the 10th INTERPRAEVENT 2004 – RIVA DeL Garda / TRIENT, May 2004, pp. VII/253-264.

Shibuya, H., Katsuki, S., Ohsumi, H., Ishikawa, N. and Mizuyama, T. (2010): Experimental study on woody debris trap performance of drift wood capturing structure, Journal of Japan Society of Erosion Control Engineering, Technical Note, Vol. 63, No. 3, pp. 34-41 (in Japanese with English abstract).

Shibuya, H., Katsuki, S., Ohsumi, H. and Ishiakwa, N. (2011): 3D-DEM simulation on trap performance of drift wood capturing structure, Journal of Japan Society of Erosion Control Engineering, Vol. 63, No. 6, pp. 13-22 (in Japanese with English abstract).

Steel Sabo Structure Committee (2009): Design manual of steel sabo structures, Sabo & Landslide Technical Center, p. 11 (in Japanese, the title is tentatively translated by the authors).

Tateishi, R., Horiguchi, T., Katsuki, S., Shima, T., Ishikawa, N. and Mizuyama, T. (2015): Experimental study on trapping sedimentation due to wooden debris by steel open dam, Proceedings of Research Meeting of Japan Society of Erosion Control Engineering, R6-03, pp. A84-85 (in Japanese , the title is tentatively translated by the authors).

Tsutsui, T., Shima. J. and Ishikawa, N. (2009): A study on debris flow trapped by steel open type sabo dam, Proceedings of Research Meeting of Japan Society of Erosion Control Engineering, No. 64, pp. 108-109 (in Japanese the title is tentatively translated by the authors).

Yamaguchi, M., Kokuryo, H. and Mizuyama. T. (2011): Excavation of debris flow trapped by steel open type sabo dam in Hachimantani river, Proceedings of Research Meeting of Japan Society of Erosion Control Engineering, No. 66, pp. 494-495 (in Japanese, the title is tentatively translated by the authors).

Yoshida, K., Yamaguchi, M. and Mizuyama, T. (2011): Field survey on the capture of debris flow with steel open sabo dams, Journal of Japan Society of Erosion Control Engineering, Technical Note, Vol. 63, No. 5, pp. 43-46 (in Japanese with English abstract).

Yoshida, K., Shima, J., Kawamura, T., Yamaguchi, M., Inoue, R. and Kokuryo, H. (2012): A survey on corrosion of steel sabo structures due to volcanic gas, Proceedings of Research Meeting of Japan Society of Erosion Control Engineering, No. 67, pp. 74-75(in Japanese, the title is tentatively translated by the authors).

Received: 8 August, 2015
Accepted: 22 January, 2016